The Roles of *ATF3*, an Adaptive-Response Gene, in High-Fat-Diet-Induced Diabetes and Pancreatic β-Cell Dysfunction

Erik J. Zmuda, Ling Qi, Michael X. Zhu, Raghavendra G. Mirmira, Marc R. Montminy, and Tsonwin Hai

Molecular, Cellular and Developmental Biology Program (E.J.Z., M.X.Z., T.H.), Department of Molecular and Cellular Biochemistry (E.J.Z., T.H.), Center for Molecular Neurobiology (E.J.Z., M.X.Z., T.H.), Department of Neuroscience (M.X.Z.), Ohio State University, Columbus, Ohio 43210; Division of Nutritional Science (L.Q.), Cornell University, Ithaca, New York 14853; Herman B. Wells Center for Pediatric Research (R.G.M.), Department of Pediatrics, Indiana University School of Medicine, Indianapolis, Indiana 46202; and Clayton Foundation Laboratories for Peptide Biology (L.Q., M.R.M.), Salk Institute for Biological Studies, La Jolla, California 92037

Most people with type 2 diabetes (T2D) have reduced β-cell mass, and apoptosis is a key factor for this reduction. Previously, we showed that *ATF3*, an adaptive-response gene, is induced by various stress signals relevant to T2D, such as high glucose and high fatty acid. Because *ATF3* is proapoptotic in β-cells, we tested the hypothesis that *ATF3* plays a detrimental role and contributes to the development of T2D. We compared wild-type (WT) and *ATF3* knockout (KO) mice in an animal model for T2D, high-fat diet-induced diabetes. We also used INS-1 β-cells and primary islets to analyze the roles of *ATF3* in β-cell function, including insulin gene expression and glucose-induced insulin secretion. Surprisingly, WT mice performed better in glucose tolerance test than KO mice, suggesting a protective, rather than detrimental, role of *ATF3*. At 12 wk on high-fat diet, no β-cell apoptosis was observed, and the WT and KO mice had comparable β-cell areas. However, *ATF3* deficiency significantly reduced serum insulin levels in the KO mice without affecting insulin sensitivity, suggesting reduced β-cell function in the KO mice. Analyses using INS-1 cells and primary islets support the notion that this defect is due, at least partly, to reduced insulin gene transcription in the KO islets without detectable reduction in glucose-induced calcium influx, a critical step for insulin secretion. In conclusion, our results support a model in which, before apoptosis becomes obvious, expression of *ATF3* can be beneficial by helping β-cells to cope with higher metabolic demand. **(*Molecular Endocrinology* 24: 1423–1433, 2010)**

Although classically referred to as non-insulin-dependent diabetes mellitus, type 2 diabetes (T2D) is a dual disease of insulin deficiency and peripheral insulin resistance (Refs. 1 and 2 and reviews in Refs. 3–9). It is well established that T2D develops only after the pancreatic β-cells fail to produce enough insulin to meet the metabolic demand (reviews in Ref. 4 and Refs. 6–8). This failure is a consequence of reduction in β-cell functional mass: a combination of reduced mass and function. At the early stage of T2D development, β-cell mass increases through compensatory mechanisms that include mainly hypertrophy but also moderate replication and neogenesis. However, over time, β-cells are induced to undergo apoptosis by various factors/mechanisms, including extracellular factors such as high concentrations of lipid and glucose and intracellular mechanisms such as mitochondrial dysfunction, triglyceride/free fatty acid cycling dysfunction, reactive oxygen species, endoplasmic reticulum (ER) stress, and amyloid plaque deposits (for reviews, see Refs. 7, 8 and 10). Eventually, apoptosis outpaces the

ISSN Print 0888-8809 ISSN Online 1944-9917
Printed in U.S.A.

doi: 10.1210/me.2009-0463 Received November 9, 2009. Accepted April 30, 2010.
First Published Online June 2, 2010

Abbreviations: ChIP, Chromatin immunoprecipitation; CRE, cAMP response element; ER, endoplasmic reticulum; GSIS, glucose-stimulated insulin secretion; HFD, high-fat diet; IPGTT, ip glucose tolerance test; KO, knockout; KRB, buffered Krebs-Ringer; Pol II, polymerase II; qPCR, quantitative PCR; qRT-PCR, quantitative RT-PCR; T2D, type 2 diabetes; TBST, Tris-buffered saline-Tween 20; TSS, transcriptional start site; WT, wild type.

compensatory mechanisms, and problems arise. Because most people with T2D have reduced β-cell mass (11), β-cell apoptosis has emerged as a key process that is dysregulated during T2D development (reviews in Refs. 7, 8, 12, and 13).

In addition to mass reduction, deterioration of β-cell function plays an important role in the pathogenesis of T2D (reviewed in Refs. 3–8). The defects in β-cell functions include loss of the first-phase insulin response (the burst of insulin secretion by β-cells within 10–15 min after meal), the abnormality in pulsatile secretion of insulin, and impairment in insulin biosynthesis (see above reviews). Recently, genome-wide association analyses aimed to identify polymorphisms that increase the risk of T2D in humans provided the exciting revelation that many T2D-risk variants affect genes regulating β-cell function and/or mass, rather than insulin signaling in the peripheral organs (reviewed in Refs. 14 and 15). Taken together, these results are consistent with a model that T2D results from the combination of gene-and-environment interactions: genetic predisposition that makes β-cells vulnerable (to metabolic demand) and environment factors that induce insulin resistance (5, 14, 16).

In this report, we describe our findings on an adaptive-response gene, activating transcription factor 3 (*ATF3*), in high-fat diet (HFD)-induced diabetes, an animal model for T2D. *ATF3* encodes a member of the ATF/cAMP response element (CRE)-binding protein family of transcription factors that share the basic region-leucine zipper DNA-binding domain and bind to the same consensus sequence TGACGTCAC *in vitro* (17). Previously, we and others showed that *ATF3* is induced in the β-cells by various stress signals relevant to T2D, including high glucose, high fatty acids, reactive oxygen species, and ER stress (18–22). Functionally, *ATF3* is proapoptotic in β-cells (19), in part by repressing the prosurvival gene *IRS2* (20). Due to the importance of β-cells in T2D development, we tested whether *ATF3* contributes to the development of T2D by comparing wild-type (WT) and *ATF3* knockout (KO) mice using a HFD model. Because of the proapoptotic role of *ATF3* in β-cells, we predicted that the KO mice would be protected, at least partially, in this model. To our surprise, the KO mice performed worse in the glucose tolerance test than the WT mice. Examination of insulin resistance and insulin deficiency led to the findings that *ATF3* enhances β-cell function. Thus, *ATF3* plays a role in both β-cell apoptosis (from previous work) and function (from this work). Results described below are consistent with a model that, before β-cell apoptosis becomes an issue, expression of *ATF3* is beneficial and helps β-cells to cope with higher metabolic demand (more in *Discussion*).

Results

The role of *ATF3* in high fat diet (HFD)-induced diabetes

To examine whether *ATF3* plays a role in the development of T2D, we compared WT and *ATF3* KO mice using an HFD-induced diabetes model. We fed 6-wk-old mice with high-fat (60%) or normal (5%) chow and monitored them for weight gain and glucose intolerance over a 16-wk period. Although the *ATF3* KO mice developed normally and exhibit no obvious phenotypes under unstressed conditions (19), they are slightly lower in body weight than the WT mice at weaning and throughout the experiments (see Supplemental Fig. 1A published on The Endocrine Society's Journals Online web site at http://mend.endojournals.org; 21.8 ± 0.38 g for WT and 19.7 ± 0.37 g for KO at 6 wk). Despite this difference, they gained weight and consumed chow at similar rates as the WT mice as shown in Supplemental Fig. 1, A and B. Consistent with induction of diabetes by HFD, both groups of mice developed hyperglycemia over time on

TABLE 1. Serum chemistry analyses of WT and *ATF3* KO mice fed HFD

	HFD			Reference range	
	***ATF3* +/+**	***ATF3* −/−**	***P* value**	**Max/min**	**Citation**
Glucose (mg/dl)	178 ± 8.4	168 ± 9.5	0.51	136/47	55, 56
(mmol/liter)	9.9 ± 0.5	9.3 ± 0.5		16.3/2.6	
NEFA (mEq/liter)	1.8 ± 0.15	1.7 ± 0.06	0.52	1.08/0.96	57, 58
(mmol/liter)	1.8 ± 0.15	1.7 ± 0.06		1.08/0.96	
Cholesterol (mg/dl)	242 ± 17.3	272 ± 13.6	0.25	121/55	55, 56
(mmol/liter)	6.2 ± 0.4	6.9 ± 0.3		3.1/1.4	
Triglycerides (mg/dl)	148 ± 13.0	119 ± 1.2	0.07	169/35	55, 56
(mmol/liter)	1.6 ± 0.1	1.3 ± 0.01		1.9/0.4	
Insulin (ng/ml)	5.4 ± 0.2	3.0 ± 0.4	0.03	1.3/0.7	58 and Fig. 2 of this report
(pmol/liter)	929 ± 34	516 ± 72		224/120	

Fasting sera collected from mice after 12 wk on HFD were analyzed (n = 6–8 mice per group). Data are expressed as means ± SEM. References ranges are from fasted mice as reported in the indicated citations. NEFA, Nonesterified fatty acid.

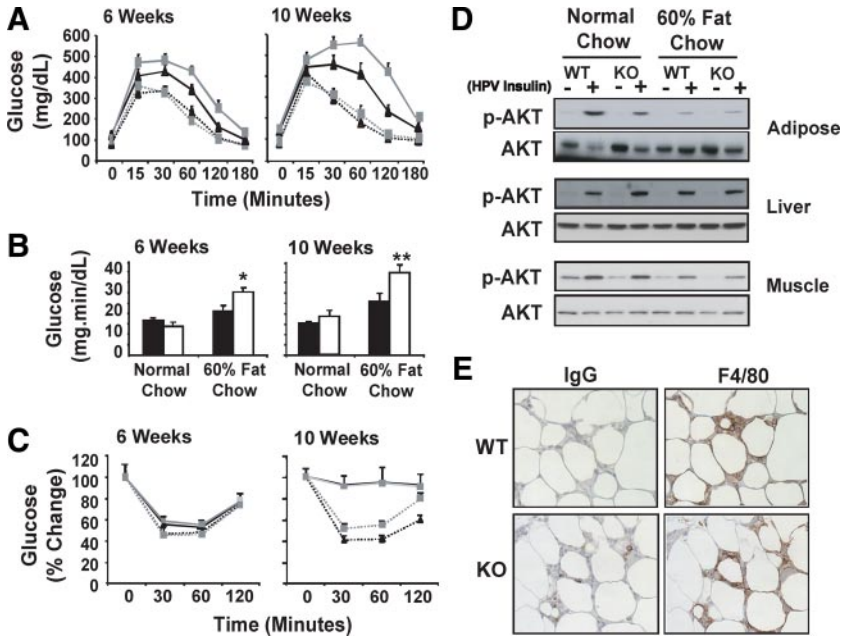

FIG. 1. *ATF3* deficiency exacerbates HFD-induced glucose intolerance. A, WT (*black lines*) and *ATF3* KO (*gray lines*) mice were placed on HFD (*solid lines*) or normal chow (*dotted lines*) and analyzed by IPGTTs at the indicated week on HFD. Shown is a representative of four independent HFD experiments (n = 10–15 per group of mice). B, Areas under the curve from panel A were shown (WT, *black bars*; KO, *white bars*). C, Mice as described in panel A were analyzed by ip insulin tolerance test at the indicated week on HFD. D, WT or KO mice fed with normal chow or HFD for 12 wk were injected with insulin via the hepatic portal vein (HPV). Epididymal fat pad, liver, and muscle were collected at 5 min after injection and analyzed by immunoblot for Akt phosphorylation. Shown is a representative blot of two independent experiments, where extracts from four mice per group were pooled for analysis. E, Epididymal fat pads from mice described in panel A were analyzed for macrophage recruitment by immunohistochemistry using antibody against F4/80. Shown are representative fields from the HFD groups with control IgG staining on adjacent sections. Presented are means ± SEM. *, $P < 0.05$; **, $P < 0.001$ KO *vs.* WT.

HFD, as indicated by increased fasting glucose levels; however, no difference was observed between the genotypes (Supplemental Fig. 1C and Table 1). Examination of serum lipid profile (nonesterified fatty acid, cholesterol, and triglyceride) also showed no statistically significant difference between the WT and KO mice on HFD (Table 1). We then challenged the mice with glucose and tested their ability to clear the glucose by ip glucose tolerance tests (IPGTT). Both groups of mice became glucose intolerant at 6 wk and 10 wk after HFD (Fig. 1A). However, to our surprise WT mice performed better, instead of worse, than the KO counterparts, as indicated by the area under the curve analysis (Fig. 1B), suggesting that *ATF3* has a protective role in maintaining glucose homeostasis under HFD. This may appear to contradict the data above that there was no difference between WT and KO mice in their fasting glucose levels over time under HFD (Supplemental Fig. 1C). One explanation is that the IPGTT assay challenged the mice for glucose handling and was thus able to discern the difference between WT and KO mice.

The difference in glucose clearance revealed by IPGTT was not due to a difference in insulin resistance, because the WT and KO mice performed similarly in insulin tolerance test (Fig. 1C) and showed similar insulin-induced Akt phosphorylation in their epididymal fat pad, liver, and muscle (Fig. 1D). We note that mice on HFD had dampened insulin-induced Akt phosphorylation in their fat pad and muscle, as compared with their counterparts under normal chow, consistent with the well-known peripheral insulin resistance induced by HFD. However, this reduction was comparable in WT and KO mice (Fig. 1D).

One exciting revelation in the obesity and diabetes field is that during obesity many immune cells (such as macrophages) infiltrate into adipose tissues, leading to elevated inflammation and systemic insulin resistance (reviewed in Refs. 23 and 24). We therefore examined inflammation in adipose tissues. As shown in Fig. 1E and Supplemental Fig. 1D, WT and KO mice had a similar macrophage infiltration in their epididymal fat pad. Furthermore, analyses of serum TNFα, a key proinflammatory cytokine in obesity (reviewed in Refs. 23 and 24), indicated no difference between the genotypes (Supplemental Fig. 1G). These, combined with similar insulin tolerance test and phospho-Akt data (above), suggest that, at the time of assay, the WT and KO mice had similar local or systemic inflammation and similar peripheral insulin signaling. Taken together, we concluded that *ATF3* has a protective role in obesity-induced diabetes; however, the protective effect is most likely not due to the reduction in inflammation or insulin resistance. This prompted us to hypothesize that *ATF3* may enhance β-cell functional mass under HFD, thus contributing to better glucose tolerance in WT than KO mice.

The role of *ATF3* in HFD-induced hyperinsulinemia

One compensatory response of β-cells to the higher metabolic demand under HFD is to produce and secrete more insulin. Analysis of fasting (Fig. 2A) and nonfasting (Fig. 2B) serum insulin levels indicated that both WT and KO mice exhibited this compensatory response: higher serum insulin levels under HFD than under normal chow. However, it was much dampened in KO mice, as indicated by the lower serum insulin levels in KO than in WT

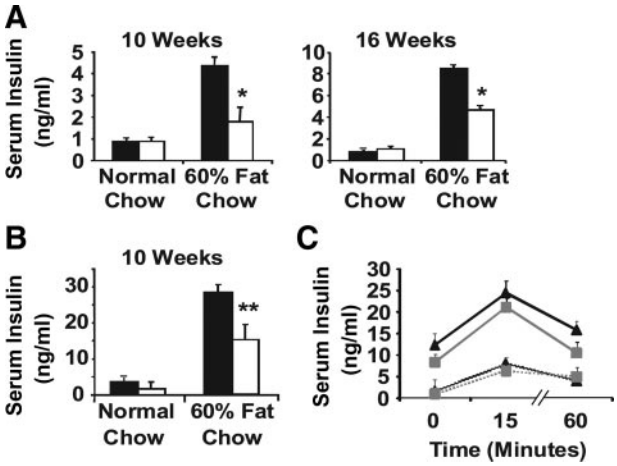

FIG. 2. *ATF3* KO mice have reduced serum insulin levels compared with WT mice on HFD. A and B, WT (*black bars*) and *ATF3* KO (*white bars*) mice fed HFD or normal chow for the indicated weeks were analyzed for fasting (panel A) and nonfasting (panel B) serum insulin. Shown is a representative of four independent HFD experiments (n = 8–10 per group of mice). C, WT (*black lines*) and *ATF3* KO (*gray lines*) fed with HFD (*solid lines*) or normal chow (*dotted lines*) for 12 wk were injected with glucose ip and analyzed for serum insulin levels at the indicated times. Shown is a representative of four independent HFD experiments (n = 5–8 per group of mice). Presented are means ± SEM. *, $P < 0.01$, **, $P < 0.005$ KO *vs.* WT. $P < 0.05$ HFD *vs.* normal chow within each genotype, except for KO mice in panel A at 10 wk.

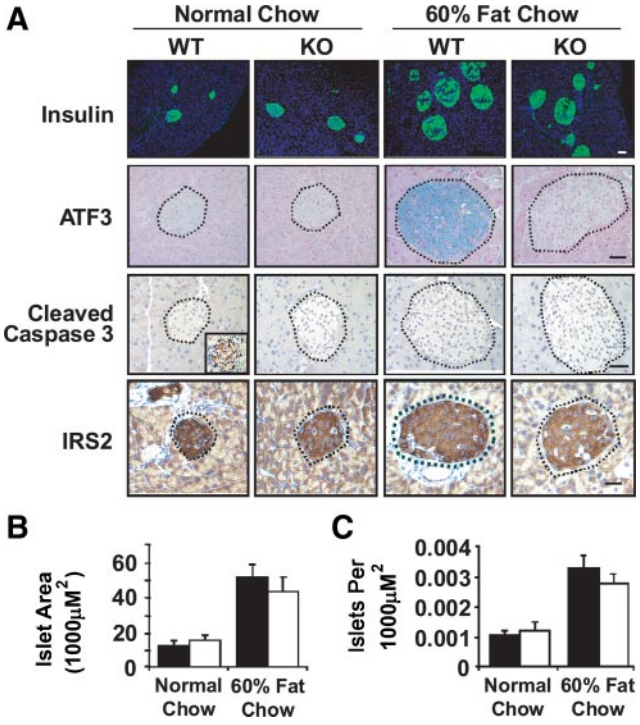

FIG. 3. WT and *ATF3* KO have comparable islet compensation under HFD**.** A, Pancreata from WT and *ATF3* KO fed HFD or normal chow for 12 wk were analyzed by immunohistochemistry with the indicated antibodies. *Bar*, 100 μm. *Inset* for cleaved caspase 3 is a positive control from a nonobese diabetic mouse. Shown are representative images. B and C, Islet size (panel B) and number (panel C) were quantified for insulin-positive cells in panel A; n = 5 mice per group; 5–10 fields from each mouse were analyzed. Presented are means ± SEM. *Black bars* indicate WT; *white bars* indicate KO.

mice. This result was observed in total four experiments with 60% fat diet and one experiment with 45% fat diet (Supplemental Fig. 2), indicating a beneficial role of *ATF3* in the compensatory increase of serum insulin under increased dietary fat content and providing an explanation for the more pronounced glucose intolerance of the KO mice. We also examined the serum insulin levels within 60 min after glucose challenge. As shown in Fig. 2C, the absolute serum insulin levels were consistently lower in the KO mice, indicating that *ATF3* deficiency attenuated the total insulin output under HFD.

To investigate the causes for the reduced serum insulin levels in KO mice, we first examined β-cell mass. As shown in Fig. 3, WT and KO mice had similar β-cell areas (Fig. 3, A and B) and islet number (Fig. 3C) under HFD. Importantly, in both groups of mice these parameters are higher under HFD than under normal chow, a well-known compensatory response under obesity (12). Immunohistochemistry showed that *ATF3* is induced in the WT islets under HFD (Fig. 3A), consistent with previous studies that *ATF3* is induced by stress signals in β cells and primary islets *in vitro* (see *Introduction*). The lack of *ATF3* signals in the KO islets (Fig. 3A) confirmed its deficiency. Because *ATF3* is proapoptotic in β-cells (19, 20), it was surprising that WT and KO islets had similar β-cell area. We thus examined activated caspase 3, an apoptosis marker, by immunohistochemistry. Figure 3A showed that no signals were detected in the WT or KO pancreata under normal chow or HFD (Fig. 3A). A side-by-side analysis of a diabetic pancreas from nonobese diabetic mice was used as a positive control for the assay (*inset*). Consistent with this finding, *IRS2*, a potent β-cell survival factor (25), was not affected in the pancreatic islets under HFD, and no difference could be discerned between the genotypes (Fig. 3A). Previously, we showed that *ATF3* represses *IRS2* expression in the INS-1 β cells (20). However, we did not observe reduction of *IRS2* signals in HFD-treated WT islets, where *ATF3* was clearly induced. We will address this apparent discrepancy in *Discussion*. Taken together, at the time of analyses (12 wk after HFD), β-cell apoptosis had not yet become a major problem. Under these conditions, *ATF3* expression appears beneficial, contributing to increased serum insulin level (Fig. 2, A and B). Because WT and KO mice had comparable islet area and number, we hypothesized that *ATF3* enhances β-cell function, specifically insulin biosynthesis, secretion, or both.

Regulation of insulin gene expression by *ATF3*

Two clues supported the notion that *ATF3* may upregulate the transcription of insulin gene. First, *ATF3* is a transcription factor; second, the insulin promoter contains a highly conserved ATF/cAMP response element

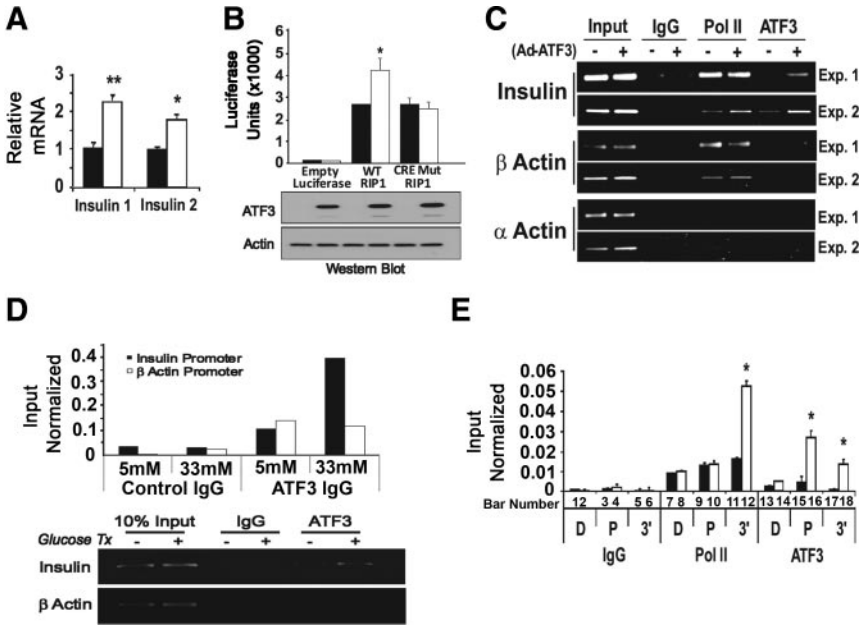

FIG. 4. *ATF3* binds to the insulin promoter and contributes to its up-regulation in INS-1 β cells. Panel A, INS-1 cells were infected with adenovirus expressing *ATF3* (Ad-ATF3, *white bar*) or βGal (Ad-βGal, *black bar*) for 36 h before qRT-PCR analysis for insulin mRNA. Shown is a representative of three experiments (Exp.). Panel B, INS-1 cells were nucleofected in triplicate with the luciferase reporters driven by the indicated promoters: WT rat insulin promoter 1 (RIP1), mutant (Mut) RIP1 promoter with changes in its ATF/CRE sequence (from TGACGTCC to TCGTGGTT), and empty promoter. All groups were infected 24 h later with adenovirus expressing *ATF3* (Ad-ATF3, *white bar*) or βGal (Ad-βGal, *black* bar) for 24 h before luciferase analysis (*top panel*). Aliquots of cellular extracts were removed before luciferase assay, pooled, and analyzed by immunoblot for *ATF3* and actin (*bottom panel*). Shown is representative of two experiments. Panel C, INS-1 cells infected with Ad-ATF3 (+) or Ad-βGal (−) were analyzed by ChIP using IgG or antibodies against *ATF3* or Pol II. Protein recruitment to insulin (I and II) promoters (around the ATF/CRE site) and two control promoters (at proximal site around TTS) were analyzed: β-actin (a β-cell gene) and α-actin (a non-β-cell gene). PCR was terminated in the linear phase of amplification, and the result from two experiments is shown. Panel D, INS-1 cells treated with 5 mM or 33 mM glucose were analyzed by ChIP using IgG or antibody against *ATF3*. Protein recruitment to insulin (1 and 2) promoters (around the ATF/CRE site) and β-actin promoter (proximal site around TTS) were analyzed. Shown is a representative of two experiments. *Top panel*, qPCR; *bottom panel*, a PCR terminated in the linear phase of amplification. Panel E, INS-1 cells infected with Ad-ATF3 (*white bars*) or Ad-βGal (*black bars*) were analyzed by ChIP using the indicated antibodies followed by qPCR. Three primer sets for different regions of the insulin gene were used: D, distal (−1200 bp from TSS); P, proximal (−200 bp from TSS), 3′, 3′-untranslated region (+1200 bp from TSS). Shown are the averages from three experiments. Presented are mean ± SEM. *, $P < 0.02$; **, $P < 0.05$, *ATF3 vs.* the corresponding controls.

(CRE) site, a potential binding site for *ATF3*, at the proximal region around −200 bp from the transcriptional start site (TSS). To test the potential of *ATF3* to regulate insulin gene expression, we examined the endogenous insulin 1 and insulin 2 mRNA levels after infecting the INS-1 β-cells with adenovirus expressing *ATF3* (Ad-ATF3) or βGal (Ad-βGal) as a control. Figure 4A shows that ectopic expression of *ATF3* increased insulin 1 and 2 steady-state mRNA levels. Reporter assay indicated the ability of *ATF3* to up-regulate the WT rat insulin 1 promoter but not the mutant promoter with changes in the ATF/CRE sequence (Fig. 4B). We also examined the ability of *ATF3* to bind to the insulin promoters using the chromatin immunoprecipitation (ChIP) assay. As shown in Fig. 4C, exogenous *ATF3* (expressed by Ad-ATF3) was recruited to the insulin promoters around the ATF/CRE site. Due to the sequence homology, the primer set does not distinguish between the two insulin promoters; thus, no distinction was made here. Control antibody (IgG) showed no signals on the insulin promoters, and control primers showed no binding of *ATF3* to the α- or β-actin promoter (Fig. 4C), which lacks recognizable ATF/CRE sites. In addition, antibody against RNA Polymerase II (Pol II) showed Pol II binding to the proximal promoter of β-actin (a β-cell gene) but not α-actin (a non-β-cell gene), further validating the ChIP procedure in this experiment. To determine whether the endogenous *ATF3* could bind to the insulin promoter, we treated INS-1 cells with high concentration of glucose (33 mM) to induce *ATF3*, followed by ChIP analyses. As shown in Fig. 4D (*bottom panel*), *ATF3* was recruited to the insulin promoter. The *top panel* shows the results of the quantitative PCR (qPCR) analyses of the ChIP signals.

The binding of *ATF3* to the insulin promoters, combined with the increased insulin mRNA levels upon *ATF3* expression, suggests (but does not prove) that *ATF3* up-regulates the transcription of insulin gene *in vivo*. Two commonly used assays for *vivo* transcription are the Pol II occupancy assay (which examines Pol II binding on the coding region downstream of the TSS) and the pre-mRNA assay (which examines the production of mRNA precursors). We carried out ChIP analysis combined with qPCR to determine Pol II occupancy on the insulin gene. As shown in Fig. 4E, Pol II antibody precipitated DNA fragment at the coding region approximately 1.5 kb downstream from the TSS (*bar 12*, detected by the primer set designated as 3′), but the control IgG did not (*bar 6*). The signal strength was 3-fold in the presence of ectopic expression of *ATF3* than that of βGal (compare *bar 12* with *bar 11*), indicating that *ATF3* enhances Pol II occupancy in the coding region. This enhancement, a surrogate measurement of *in vivo* transcription, was observed neither in the distal promoter region approximately 1.5 kb up-

stream from TSS (*bars 7* and *8*, using primer set designated as D) nor in the proximal region around the TSS (*bars 9* and *10*, using primer set designated as P), supporting the specificity of this *in vivo* transcription assay. Taken together, these results, *i.e.* increased steady-state mRNA levels, reporter activity, *in vivo* DNA binding, and *in vivo* transcription, strongly indicate that insulin is a direct target gene of *ATF3* and is up-regulated by *ATF3*.

The role of *ATF3* in primary islets

To test whether *ATF3* plays a role in insulin gene expression in primary islets, we compared WT and KO islets in the absence or presence of high concentration of glucose (33 mM) for 1 h, a condition that induces *ATF3* expression (see later in text) and is known to induce the transcription of insulin gene (26, 27). Figure 5 shows that glucose treatment increased the endogenous ATF3 protein level (panel A) and the steady-state insulin 1 and insulin 2 mRNA levels in the WT but not KO islets (panel B), indicating that *ATF3* contributes to the increased insulin expression. To test whether this is due to an increase in transcription, we analyzed insulin 2 pre-mRNA level. This pre-mRNA contains two introns, and the precursor with unspliced intron 2 has a half-life on the order of minutes (28–30). Thus, the level of this precursor, which can be assayed by RT-PCR using a primer specific to intron 2 and a primer targeted to the preceding exon, is a good indicator for transcription as demonstrated previously (29). As shown in Fig. 5C, glucose treatment increased insulin 2 pre-mRNA levels in the WT but not KO islets, supporting the notion that *ATF3* enhances insulin gene transcription. Analysis of *ATF3* mRNAs confirmed the induction of *ATF3* in WT but not KO islets, and the minus RT control showed no signals for all lanes (data not shown). Figure 5D shows the quantitation of insulin 2 pre-mRNA levels from five independent experiments. Taken together, glucose stimulation failed to increase the transcription of insulin gene in the *ATF3* KO islets, indicating that *ATF3* is a necessary factor for this process. However, this does not mean that other transcription factors are not important.

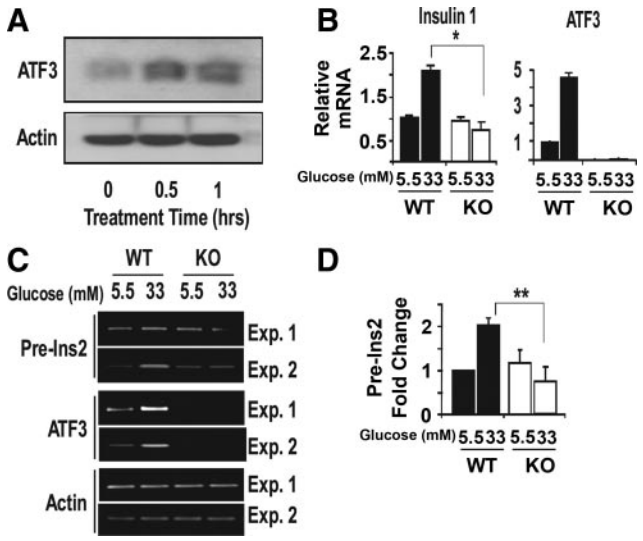

FIG. 5. *ATF3* contributes to the up-regulation of insulin gene expression in primary islets. A, Primary islets isolated from WT or KO mice were allowed to recover for 72 h in 5.5 mM glucose before 33 mM glucose treatment for the indicated time and analyzed by immunoblot for *ATF3* or actin. B, Primary islets as described in panel A were analyzed for mature insulin 1 by qRT-PCR and for *ATF3* mRNA as a control. Shown are the averages from three experiments. C, Primary islets as described in panel A were analyzed for preinsulin 2 (pre-Ins2) RNA by RT-PCR and for *ATF3* and actin mRNAs as controls. Shown are two representatives of a total of five experiments. D, Pre-Ins2 signals as obtained in panel C from five experiments were quantified. Presented are means ± SEM. *Black bars* represent WT; *white bars* represent KO. *, $P < 0.05$; **, $P < 0.006$ KO *vs.* WT with the corresponding glucose treatment. Exp., Experiment.

We next examined the intracellular insulin protein level and found that it was lower in the KO islets than in the WT islets (Fig. 6A, *left panel*). Glucose-stimulated insulin secretion (GSIS) showed that the amount of insulin in the KO supernatant was much lower than that in the WT supernatant (Fig. 6A, *right panel*). Because the KO islets had lower intracellular insulin level, the defect in GSIS could be simply a secondary effect. Alternatively, this could be a combination of reduced insulin production and reduced exocytosis. Therefore, we examined glucose-stimulated calcium influx, a key regulatory step for glucose-induced insulin exocytosis (31, 32). As shown in Fig. 6, B and C, WT and KO islets achieved similar intracellular Ca^{2+} concentration in response to glucose stimulation. The only difference was a slight elevation of the resting Ca^{2+} level (preglucose minimum) in the KO islets (Fig. 6C). The significance of this subtle difference is not clear. We also examined calcium oscillation at 25 mM or 11 mM glucose and did not observe any obvious difference (Fig. 6, D–F for 25 mM; Supplemental Fig. 3 for 11 mM). Taken together, these results suggest that the *ATF3* deficiency does not impact on calcium homeostasis to any appreciable degree.

Discussion

In summary, we investigated the roles of *ATF3*, an adaptive-response gene, in HFD-induced diabetes. Because of its proapoptotic role in β-cells, we originally hypothesized that WT mice would perform worse than KO mice in the glucose tolerance test. However, to our surprise, the result was the opposite. Further analyses indicated that, compared with WT mice, KO mice had significantly reduced serum insulin levels but no obvious difference in their insulin tolerance test. These results led to the identification of a new target gene of *ATF3*: insulin. Many

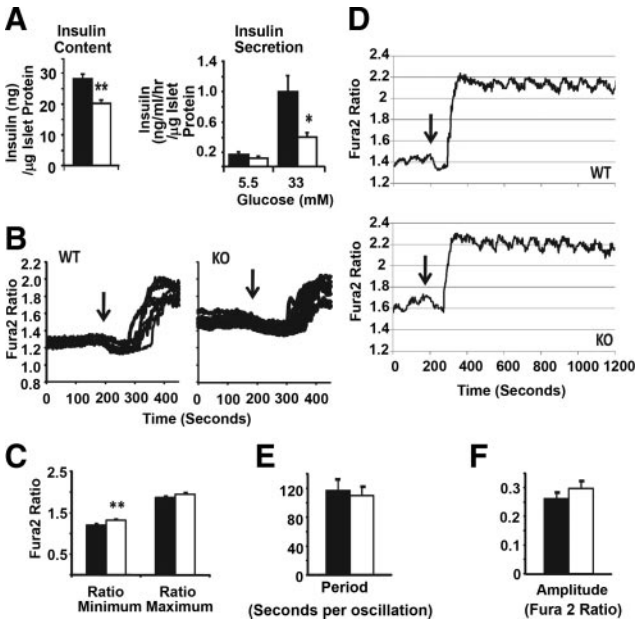

FIG. 6. *ATF3* deficiency reduces total insulin secreted by the primary islets upon glucose challenge but does not affect calcium influx or oscillation. A, Primary islets from WT (*black bars*) and *ATF3* KO (*white bars*) mice were analyzed for their intracellular insulin content using ELISA (*left panel*) or glucose-induced insulin secretion by measuring insulin in the supernatant (*right panel*). Shown are representatives of three independent experiments. For each experiment, 15 islets were pooled for assay, and five to 10 pools of islets per genotype were analyzed to generate the data. B, Primary islets were allowed to recover for 24 h in 5.5 mM glucose before fura-2 loading and analyzed by Ca^{2+} imaging for glucose-stimulated (from 2.5 mM to 25 mM glucose) change in intracellular Ca^{2+} concentration. Islets (n = 100) were analyzed for each group, and the experiments were repeated three times. Shown are traces of extracellular Ca^{2+} influx from 20 islets. *Arrows* indicate the expected Ca^{2+} sequestration by ER before influx. C, Fura-2 340/380 ratios from islets in panel B were combined to obtain the average preglucose minimum and postglucose maximum. Shown are representative of three experiments (n =100 islets). D, A representative trace of glucose-stimulated Ca^{2+} influx and oscillations from islets in panel B was shown. *Arrows* are as indicated in panel B. E and F, Period (panel E) and amplitude (panel F) of glucose-stimulated calcium oscillation from panel D were quantified (n = 100 islets). Presented are means ± SEM. *, $P < 0.05$; **, $P < 0.01$ KO *vs.* WT.

target genes of *ATF3* have been identified, including various inflammatory genes, cell cycle-regulatory genes, and genes involved in cancer development (reviewed in Ref. 33). Here, we discuss a few target genes that are identified in cell types relevant to this study: β-cells, hepatocytes, adipocytes, and macrophages. We do not include muscle, a major insulin-responsive tissue, for discussion, because *ATF3* was not detected in the muscle under HFD (Supplemental Fig. 1F) and because no myocyte target genes of *ATF3* have been reported. In β-cells, *ATF3* was shown to repress *IRS2* (20), a potent prosurvival factor in β-cells (25), under the cytokine or ER stress. In this study, we did not observe any reduction of *IRS2* in the WT islets under HFD, which showed obvious *ATF3* induction (Fig. 3A). One explanation is that the consequence of *ATF3* induction is context dependent: the HFD-induced islets may lack certain cofactors for *ATF3* to repress the *IRS2* promoter; alternatively, some inhibitory factors may be present to counteract the effect of *ATF3*, leading to the lack of *IRS2* repression. *ATF3* was recently shown to up-regulate several proinflammatory genes in islets under stress conditions relevant to transplantation, such as cytokines, hypoxia, and isolation stress (34). However, it is not clear whether the HFD stress used in this study also induces these proinflammatory genes in the islets. In neonatal hepatocytes, *ATF3* was shown to repress the expression of *PEPCK* gene (35), which encodes a gluconeogenic enzyme. If *PEPCK* gene is repressed by *ATF3* under HFD, this response could be another beneficial effect of *ATF3* for WT mice to handle glucose. In adipocytes, *ATF3* was shown to repress adiponectin (36, 37), an insulin-sensitizing adipokine (38). However, we did not observe lower insulin sensitivity in the WT mice than in the KO. One potential explanation is that *ATF3* is multifunctional, and its other functions counteract this undesired adiponectin-repressing action. As an example, in macrophages *ATF3* represses the expression of several proinflammatory genes (including *IL6* and *IL1β*) (39–41), a function that will dampen the inflammatory response both locally and systemically and thus provide beneficial effects. Clearly, a tissue-selective KO of *ATF3* will be required to dissect the potential roles of *ATF3* in various tissues in the HFD stress model.

As described in *Results*, at the time of analyses (12 wk on HFD) β-cell apoptosis was not yet a problem, as evidenced by the lack of caspase 3 activation (Fig. 3A). This supposition is also supported by two other observations. First, neither WT nor KO had developed insulin resistance in their liver: as shown in Fig. 1D, intraportal injection of insulin induced Akt phosphorylation in both WT and KO mice, and the level of induction was comparable to that in their counterparts fed with normal chow. Second, the mice still had normal compensatory response, *i.e.* increased β-cell mass (Fig. 3, B and C). Thus, the mice were at relatively early stages of obesity-induced diabetes. In the absence of apparent β-cell apoptosis, the effects of *ATF3* to improve β-cell function predominate, leading to the better performance of WT mice than KO.

The lack of apoptosis in the WT islets indicates that induction of *ATF3* does not necessarily lead to β-cell apoptosis, despite its potential to do so. Considering the context-dependent nature of *ATF3*, this is not surprising. One example of the context-dependency of *ATF3* is its dichotomous role in breast cancer cells: it enhances stress-induced apoptosis in untransformed cells but protects malignant cancer cells from stress-induced detrimental effects (42). The fact that β-cells did not undergo apopto-

sis at 12 wk on HFD allowed us to investigate *ATF3* for its potential functions other than proapoptosis. This led to the identification of a role for *ATF3* in β-cell function. Our studies primarily focused on the transcription of insulin gene. Previously, glucose was demonstrated to increase insulin biosynthesis at the transcriptional, post-transcriptional, and translational levels (reviews in Refs. 43 and 44). At the transcriptional level, the increase has been shown to occur within minutes after glucose stimulation (26). However, due to the long half-life of the mature insulin mRNAs (30), transcriptional regulation is thought to be a mechanism to increase insulin production in response to long-term, rather than acute, glucose stimulation (43, 44). In light of this view, we interpret that the decreased serum insulin levels in the KO mice on HFD, a long-term stress model, was due, at least partly, to the decrease in insulin gene transcription in the *ATF3*-deficient β-cells. We note that the KO mice did not develop diabetes under normal chow, despite their defect in glucose-induced insulin gene transcription. We posit that, under normal chow, the postprandial increase in serum glucose levels is an acute stimulation, in which transcriptional regulation is not the main mechanism to increase insulin production (see above). Thus, the deficiency of *ATF3* did not pose major problems, and no diabetic phenotypes were observed in the KO mice. Consistent with this supposition, *ATF3* in the WT islets under normal chow was barely detectable (Fig. 3A). Thus, *ATF3* is unlikely to be the major transcription factor regulating insulin gene transcription under normal chow. In this context, it is important to note that *ATF3* is a stress-inducible gene, and its levels under normal conditions are very low, mostly undetectable. Thus, for most of the phenotypes reported for the *ATF3* KO mice, in the literature and in our own experience, they become obvious only under stress conditions. Thus, the lack of diabetic phenotypes of the KO mice on normal chow is consistent with the behavior of this mouse line.

In addition to insulin gene transcription, *ATF3* deficiency affected GSIS (Fig. 6A). Because the KO islets had reduced insulin content, the reduction in insulin release could be simply a secondary effect. Alternatively, the KO islets may also have impaired secretory process. We found that glucose-induced calcium response, the triggering step during the secretory process, was not detectably different between WT and KO islets. However, we did not address other steps regulating insulin secretion, which include the amplification step that amplifies the action of Ca^{2+} and the exocytosis step that is composed of granule recruitment, docking, priming, and fusion (45). In addition, we did not address the issue of calcium-independent secretion (45). Further investigation is required to address these issues and is beyond the scope of this report.

The novelty of our findings is that they linked *ATF3*, a proapoptotic gene, to β-cell function. Because *ATF3* is an adaptive-response gene induced by many stress signals encountered by β-cells during the development of T2D, these results have significant implications. Of particular interest is the β-cell exhaustion concept proposed by Leahy (46, 47) and Butler and associates (48). According to this concept, hyperstimulation of β-cells to produce and release insulin is a nonsustainable event; β-cells become exhausted, and eventually dysfunction/failure ensues (reviews in Refs. 3 and 4). A key point of this concept is that hyperglycemia is a stimulus for β-cell dysfunction. In lieu of this concept, we propose the following speculative model to explain the roles of *ATF3* in T2D. At the early stage of disease development, stress-induced *ATF3* helps the β-cells to cope with high metabolic demands, at least in part, by increasing insulin gene transcription. However, this adaptation or coping mechanism comes with a cost, because *ATF3* is a double-edged sword. Its detrimental, proapoptotic function comes into play when proper cellular context emerges after prolonged β-cell overwork. Clearly, this is a speculation, and more investigation is required to test this model.

In conclusion, *ATF3* regulates β-cell apoptosis (34) and function (present report), two important aspects of β-cells in T2D development. Because *ATF3* is an adaptive-response gene the expression of which can be modulated by many signals, our work identified a molecular target for the environmental factors and potential therapeutic agents to impact β-cells and T2D development.

Materials and Methods

Animals and dietary treatment

WT and *ATF3* KO C57BL/6 mice were housed under conventional conditions and cared for according to Ohio State University Laboratory Animal Resources guidelines. *ATF3* KO mice were described previously (19). At 6 wk of life, male mice were divided into groups of 10–15 and fed either normal chow (Harlan Bioproducts for Science, Inc., Indianapolis, IN; no. 8640) or a HFD (Research Diets, New Brunswick, NJ) consisting of 10% (no. D12450B), 45% (no. D12451), or 60% (no. D12492) fat for up to 16 wk.

Glucose tolerance tests, insulin tolerance test, ELISA, and serum chemistry assays

Glucose tolerance tests were performed on 16 h fasted mice by ip injection with 2 g of glucose/kg of body weight, and insulin tolerance tests were performed on 4 h fasted mice by ip injection with 0.75 U of insulin/kg of body weight. For both assays, blood samples were obtained from the snipped tail and analyzed using an Ascensia Contour portable glucometer at 15, 30, 60, 120, and 180 min after injection. Serum from nonfasting or 16 h

fasted mice were obtained via tail vein bleeds and analyzed as follow: insulin and TNFα levels measured by ELISA (Linco Research, Inc., St. Charles, MO), nonesterified fatty acid by the acetyl-coenzyme A synthetase-acetyl-coenzyme A oxidase method (Wako Pure Chemical Industries, Ltd., Osaka, Japan), and glucose, triglyceride, and cholesterol at the Ohio State University Clinical Chemistry Laboratory.

Cell culture, adenoviruses, and luciferase assay

INS-1 and INS-r3 cells were grown as previously described (49). Both cell lines were used for mRNA analysis and ChIP and yielded consistent results. Unless otherwise indicated, all cells were cultivated with standard humidified cell culture conditions. Adenoviruses were constructed using the Invitrogen Gateway technology (Invitrogen, Carlsbad, CA) and purified by cesium chloride ultracentrifugation (50). For luciferase experiments, INS cells were transfected in triplicate with a Nucleofector I (Amaxa, Gaithersburg, MD) using Solution V, Program T-27, and 4 μg of DNA per 2.5×10^6 cells. The nucleofection efficiency was approximately 25%.

Islet isolation

Islets were isolated from adult mice as previously described (20, 51, 52) and cultured in RPMI 1640 supplemented with 10% fetal bovine serum and 1% penicillin/streptomycin. The islets were allowed to recover for 72 h at 27 C in a humidified cell culture incubator before use.

RNA analyses and ChIP assay

Total RNA was isolated using Trizol (Invitrogen). cDNA was made from 5 μg of total RNA subjected to a reverse transcriptase (Promega Corp., Madison, WI) reaction primed with either random hexamer or oligo dT. cDNA was then subjected to RT-PCR or quantitative RT-PCR (qRT-PCR) in triplicate using the Bio-Rad iQ SYBR Green Supermix and a iCycler Thermocycler (Bio-Rad Laboratories, Inc., Hercules, CA). The cycling condition used for qRT-PCR was: one cycle of 95 C for 5 min; 50 cycles of 95 C 30 sec, 55 C 30 sec, 72 C 30 sec (Plate Read); one cycle of melting curve (Continuous Plate Read); 4 C infinite hold. qRT-PCR signals were standardized against actin mRNAs. ChIP assay was carried out as described previously (53) and detailed in the Supplemental Methods. All PCR primers are listed in Supplemental Table 1.

Immunoblot and immunohistochemistry

Immunoblots were performed on 50–100 μg of protein extracts subjected to 12% acrylamide SDS-PAGE and transferred to a polyvinylidene difluoride membrane (Millipore Corp., Bedford, MA). Membranes were blocked with a 5% milk TBST buffer (5% powdered milk; 50 mM Tris-HCl, pH 6.8; 150 mM NaCl; 0.05% Tween 20) before overnight incubation with the indicated antibody. Membranes were then washed three times with TBST and incubated with a horseradish peroxidase-conjugated secondary antibody for 1 h. Membranes were again washed three times before chemiluminescent development (Roche, Indianapolis, IN). Immunohistochemistry was performed on paraffin-embedded tissue samples after xyline deparaffin incubation and rehydration through ethanol into water. Antigen retrieval was used for the following antigens: caspase (citrate buffer, 60 C incubator for 4 h); F4/80 (citrate buffer in steamer for 1 h); *IRS2* (citrate buffer, boiling for 25 min). Before antibody incubation, slides were blocked in TBST supplemented with 5% Normal Goat Serum (Vector Laboratories, Inc., Burlingame, CA). The antibodies are the following: anti-*ATF3* (Santa Cruz Biotechnology, Inc., Santa Cruz, CA), antiactin (Sigma, St. Louis, MO), anti-AKT (Cell Signaling Technology, Danvers, MA), anti-phospho-AKT (Cell Signaling), anticleaved caspase 3 (Cell Signaling Technology), antiinsulin (DAKO Corp., Carpinteria, CA), anti-F4/80 (Caltag Laboratories, Inc., Buckingham, UK), and anti-*IRS2* (Cell Signaling Technology).

Glucose-stimulated calcium influx

Changes in intracellular Ca^{2+} levels were monitored by Ca^{2+} imaging as previously described (54). Briefly, islets were loaded with 2 μM fura-2 AM in a HEPES-buffered Krebs-Ringer (KRB) solution containing 2.5 mM glucose at 37 C for 60 min. After loading, the islets were washed, transferred to a small volume chamber (MatTek Corp., Ashland, MA) and placed on the stage of a Nikon TE200 fluorescence microscope (Nikon, Melville, NY). Islets were perfused with the KRB solution (2.5 mM glucose) using a peristaltic pump (Gilson, Middleton, WI) for 15 min before data collection was initiated. The perfusate was heated using an in-line heater (Harvard Apparatus, Inc., Natick, MA) to maintain the chamber solution temperature at approximately 35 C throughout the experiment. The islets were excited alternately at 340 nm and 380 nm, and the fluorescence emission was excited at 510 nm through a $\times$20 objective collected using an ORCA-ER camera (Hamamatsu, Bridgewater, NJ). Paired images were recorded every 5 sec. After recording the baseline in 2.5 mM glucose for approximately 3 min, a KRB solution containing 25 mM glucose was perfused for another 20 min. The glucose-stimulated Ca^{2+} influx in individual islets was defined as the difference between fura-2 ratio (340/380 nm fluorescence) in 25 mM *vs.* 2.5 mM glucose for regions of interest defined by the contour of the islets in the fluorescence images. Data were analyzed with IP Lab software version 4.0 (Scanalytics, Inc., Fairfax, VA).

Image analysis and statistics

Immunohistochemistry and densitometry analysis was done using the NIH ImageJ Software (version 1.41a). All quantitative data are expressed as means $\pm$ SEM, and statistical analyses are made by Student's *t* test (unpaired, two tailed).

Acknowledgments

We thank Shawn Behan for maintaining the mouse colonies and genotyping the mice. We also thank Catherine Powell for assisting proofing and revising this manuscript.

Address all correspondence and requests for reprints to: Tsonwin Hai, Room 174 Rightmire Hall, 1060 Carmack Road, Ohio State University, Columbus, Ohio 43210. E-mail: hai.2@osu.edu.

This work was supported by National Institutes of Health (NIH) Grant RO1 DK064938 and American Recovery and Reinvestment Act Supplemental Award DK 064938-S1 (to T.H.), and NIH Grants DK60581 (to R.G.M.), DK081654 (to M.X.Z), and P30-NS045758 (to Ohio State Neuroscience Center Core Grant).

Disclosure Summary: The authors have nothing to disclose.

References

1. **Weir G** 1982 Non-insulin-dependent diabetes mellitus: interplay between β-cell inadequacy and insulin resistance. Am J Med 73: 4651–4664
2. **Ward WK, Beard JC, Porte Jr D** 1986 Clinical aspects of islet B-cell function in non-insulin-dependent diabetes mellitus. Diabetes Metab Rev 2:297–313
3. **Leahy JL** 2005 Pathogenesis of type 2 diabetes mellitus. Arch Med Res 36:197–209
4. **Leahy J** 2005 β-Cell dysfunction in type 2 diabetes mellitus. In: Kahn C, Weir G, King G, Jacobson A, Moses A, Smith R, eds. Joslin's diabetes mellitus. 14th ed. Philadelphia: Lippincott Williams & Wilkins; 449–461
5. **Polonsky KS, Sturis J, Bell GI** 1996 Non-insulin-dependent diabetes mellitus—a genetically programmed failure of the β cell to compensate for insulin resistance. N Engl J Med 334:777–783
6. **Kahn SE** 2001 The importance of β-cell failure in the development and progression of type 2 diabetes. J Clin Endocrinol Metab 86: 4047–4058
7. **Prentki M, Nolan CJ** 2006 Islet β cell failure in type 2 diabetes. J Clin Invest 116:1802–1812
8. **Rhodes CJ** 2005 Type 2 diabetes—a matter of β-cell life and death? Science 307:380–384
9. **Maedler K, Donath MY** 2004 β-Cells in type 2 diabetes: a loss of function and mass. Horm Res 62(Suppl 3):67–73
10. **Eizirik DL, Cardozo AK, Cnop M** 2008 The role for endoplasmic reticulum stress in diabetes mellitus. Endocr Rev 29:42–61
11. **Butler AE, Janson J, Bonner-Weir S, Ritzel R, Rizza RA, Butler PC** 2003 β-Cell deficit and increased $\hat{I}^2$-cell apoptosis in humans with type 2 diabetes. Diabetes 52:102–110
12. **Butler AE, Janson J, Soeller WC, Butler PC** 2003 Increased β-cell apoptosis prevents adaptive increase in β-cell mass in mouse model of type 2 diabetes: evidence for role of islet amyloid formation rather than direct action of amyloid. Diabetes 52:2304–2314
13. **Pick A, Clark J, Kubstrup C, Levisetti M, Pugh W, Bonner-Weir S, Polonsky KS** 1998 Role of apoptosis in failure of β-cell mass compensation for insulin resistance and β-cell defects in the male Zucker diabetic fatty rat. Diabetes 47:358–364
14. **McCarthy MI** 2009 What will genome-wide association studies mean to the clinical endocrinologist? J Clin Endocrinol Metab 94: 2245–2246
15. **Florez JC** 2008 Newly identified loci highlight β cell dysfunction as a key cause of type 2 diabetes: where are the insulin resistance genes? Diabetologia 51:1100–1110
16. **Pimenta W, Korytkowski M, Mitrakou A, Jenssen T, Yki-Jarvinen H, Evron W, Dailey G, Gerich J** 1995 Pancreatic β-cell dysfunction as the primary genetic lesion in NIDDM. Evidence from studies in normal glucose-tolerant individuals with a first-degree NIDDM relative. JAMA 273:1855–1861
17. **Hai T, Wolfgang CD, Marsee DK, Allen AE, Sivaprasad U** 1999 ATF3 and stress responses. Gene Expression 7:321–335
18. **Busch AK, Cordery D, Denyer GS, Biden TJ** 2002 Expression profiling of palmitate- and oleate-regulated genes provides novel insights into the effects of chronic lipid exposure on pancreatic β-cell function. Diabetes 51:977–987
19. **Hartman MG, Lu D, Kim ML, Kociba GJ, Shukri T, Buteau J, Wang X, Frankel WL, Guttridge D, Prentki M, Grey ST, Ron D, Hai T** 2004 Role for activating transcription factor 3 in stress-induced β-cell apoptosis. Mol Cell Biol 24:5721–5732
20. **Li D, Yin X, Zmuda EJ, Wolford CC, Dong X, White MF, Hai T** 2008 The repression of IRS2 gene by ATF3, a stress-inducible gene, contributes to pancreatic ß-cell apoptosis. Diabetes 57:635–644
21. **Cunha DA, Hekerman P, Ladrière L, Bazarra-Castro A, Ortis F, Wakeham MC, Moore F, Rasschaert J, Cardozo AK, Bellomo E, Overbergh L, Mathieu C, Lupi R, Hai T, Herchuelz A, Marchetti P, Rutter GA, Eizirik DL, Cnop M** 2008 Initiation and execution of lipotoxic ER stress in pancreatic β-cells. J Cell Sci 121:2308–2318
22. **Allen-Jennings AE, Hartman MG, Kociba GJ, Hai T** 2001 The roles of ATF3 in glucose homeostasis: a transgenic mouse model with liver dysfunction and defects in endocrine pancreas. J Biol Chem 276:29507–29514
23. **Savage DB, Petersen KF, Shulman GI** 2007 Disordered lipid metabolism and the pathogenesis of insulin resistance. Physiol Rev 87: 507–520
24. **Guilherme A, Virbasius JV, Puri V, Czech MP** 2008 Adipocyte dysfunctions linking obesity to insulin resistance and type 2 diabetes. Nat Rev Mol Cell Biol 9:367–377
25. **Rhodes CJ, White MF** 2002 Molecular insights into insulin action and secretion. Eur J Clin Invest 32(Suppl 3):3–13
26. **Leibiger B, Moede T, Schwarz T, Brown GR, Köhler M, Leibiger IB, Berggren PO** 1998 Short-term regulation of insulin gene transcription by glucose. Proc Natl Acad Sci USA 95:9307–9312
27. **Nielsen DA, Welsh M, Casadaban MJ, Steiner DF** 1985 Control of insulin gene expression in pancreatic β-cells and in an insulin-producing cell line, RIN-5F cells. I. Effects of glucose and cyclic AMP on the transcription of insulin mRNA. J Biol Chem 260:13585–13589
28. **Evans-Molina C, Garmey JC, Ketchum R, Brayman KL, Deng S, Mirmira RG** 2007 Glucose regulation of insulin gene transcription and pre-mRNA processing in human islets. Diabetes 56:827–835
29. **Iype T, Francis J, Garmey JC, Schisler JC, Nesher R, Weir GC, Becker TC, Newgard CB, Griffen SC, Mirmira RG** 2005 Mechanism of insulin gene regulation by the pancreatic transcription factor Pdx-1: application of pre-mRNA analysis and chromatin immunoprecipitation to assess formation of functional transcriptional complexes. J Biol Chem 280:16798–16807
30. **Wang J, Shen L, Najafi H, Kolberg J, Matschinsky FM, Urdea M, German M** 1997 Regulation of insulin preRNA splicing by glucose. Proc Natl Acad Sci USA 94:4360–4365
31. **Henquin JC** 2000 Triggering and amplifying pathways of regulation of insulin secretion by glucose. Diabetes 49:1751–1760
32. **Henquin JC** 2009 Regulation of insulin secretion: a matter of phase control and amplitude modulation. Diabetologia 52:739–751
33. **Thompson MR, Xu D, Williams BR** 2009 ATF3 transcription factor and its emerging roles in immunity and cancer. J Mol Med 87:1053–1060
34. **Zmuda EJ, Viapiano M, Grey ST, Hadley G, Garcia-Ocana A, Hai T** 28 March 2010 Deficiency of ATF3, an adaptive-response gene, protects islets and ameliorates inflammation in a syngeneic mouse transplanation model. Diabetologia DOI: 10.1007/s00125-010-1696-x
35. **Allen-Jennings AE, Hartman MG, Kociba GJ, Hai T** 2002 The roles of ATF3 in liver dysfunction and the regulation of phosphoenolpyruvate carboxykinase gene expression. J Biol Chem 277:20020–20025
36. **Kim HB, Kong M, Kim TM, Suh YH, Kim WH, Lim JH, Song JH, Jung MH** 2006 NFATc4 and ATF3 negatively regulate adiponectin gene expression in 3T3–L1 adipocytes. Diabetes 55:1342–1352
37. **Qi L, Saberi M, Zmuda E, Wang Y, Altarejos J, Zhang X, Dentin R, Hedrick S, Bandyopadhyay G, Hai T, Olefsky J, Montminy M** 2009 Adipocyte CREB promotes insulin resistance in obesity. Cell Metab 9:277–286
38. **Kadowaki T, Yamauchi T, Kubota N, Hara K, Ueki K, Tobe K** 2006 Adiponectin and adiponectin receptors in insulin resistance, diabetes, and the metabolic syndrome. J Clin Invest 116:1784–1792
39. **Khuu CH, Barrozo RM, Hai T, Weinstein SL** 2007 Activating transcription factor 3 (ATF3) represses the expression of CCL4 in murine macrophages. Mol Immunol 44:1598–1605
40. **Gilchrist M, Thorsson V, Li B, Rust AG, Korb M, Roach JC, Kennedy K, Hai T, Bolouri H, Aderem A** 2006 Systems biology approaches identify ATF3 as a negative regulator of Toll-like receptor 4. Nature 441:173–178
41. **Whitmore MM, Iparraguirre A, Kubelka L, Weninger W, Hai T, Williams BR** 2007 Negative regulation of TLR-signaling pathways by activating transcription factor-3. J Immunol 179:3622–3630

42. **Yin X, DeWille JW, Hai T** 2008 A potential dichotomous role of ATF3, an adaptive-response gene, in cancer development. Oncogene 27:2118–2127
43. **German M** 2005 Genetic regulation of islet function. In: Kahn CR, Weir GC, King G, Jacobson AM, Moses AC, Smith RJ, eds. Joslin's diabetes mellitus. 14th ed. Philadelphia: Lippincott Williams & Wilkins; 53–64
44. **Rhodes CJ, Shoelson SE, Halban PA** 2005 Insulin biosynthesis, processing and chemistry. In: Kahn CR, Weir GC, King G, Jacobson AM, Moses AC, Smith RJ, eds. Joslin's diabetes mellitus. 14th ed. Philadelphia: Lippincott Williams & Wilkins; 65–82
45. **Henquin J-C** 2005 Cell biology of insulin secretion. In: Kahn CR, Weir GC, King G, Jacobson AM, Moses AC, Smith RJ, eds. Joslin's diabetes mellitus. 14th ed. Philadelphia: Lippincott Williams & Wilkins; 84–107
46. **Leahy J** 1996 β-Cell dysfunction with chronic hyperglycemia: the "overworked β-cell" hypothesis. Diabetes Rev 4:298–319
47. **Leahy JL** 2000 Detrimental effects of chronic hyperglycemia in the pancreatic β-cell. In: LeRoth D, Talyor SI, Olefsky JM, eds. Diabetes mellitus: a fundamental and clinical text. 2nd ed. Philadelphia: Lippincott Williams & Wilkins; 115–125
48. **Laedtke T, Kjems L, Pørksen N, Schmitz O, Veldhuis J, Kao PC, Butler PC** 2000 Overnight inhibition of insulin secretion restores pulsatility and proinsulin/insulin ratio in type 2 diabetes. Am J Physiol Endocrinol Metab 279:E520–E528
49. **Hohmeier HE, Mulder H, Chen G, Henkel-Rieger R, Prentki M, Newgard CB** 2000 Isolation of INS-1-derived cell lines with robust ATP-sensitive K+ channel-dependent and -independent glucose-stimulated insulin secretion. Diabetes 49:424–430
50. **Southgate TD, Kingston PA, Castro MG** 2000 Gene transfer into neural cells in vitro using adenoviral vectors. In: Current protocols in neuroscience. New York: John Wiley & Sons, Inc.; 4.23.1–4.23.40
51. **Grey ST, Longo C, Shukri T, Patel VI, Csizmadia E, Daniel S, Arvelo MB, Tchipashvili V, Ferran C** 2003 Genetic engineering of a suboptimal islet graft with A20 preserves β cell mass and function. J Immunol 170:6250–6256
52. **Salvalaggio PR, Deng S, Ariyan CE, Millet I, Zawalich WS, Basadonna GP, Rothstein DM** 2002 Islet filtration: a simple and rapid new purification procedure that avoids Ficoll and improves islet mass and function. Transplantation 74:877–879
53. **Lu D, Wolfgang CD, Hai T** 2006 Activating transcription factor 3, a stress-inducible gene, suppresses Ras-stimulated tumorigenesis. J Biol Chem 281:10473–10481
54. **Jahanshahi P, Wu R, Carter JD, Nunemaker CS** 2009 Evidence of diminished glucose stimulation and endoplasmic reticulum function in nonoscillatory pancreatic islets. Endocrinology 150:607–615
55. **Boehm O, Zur B, Koch A, Tran N, Freyenhagen R, Hartmann M, Zacharowski K** 2007 Clinical chemistry reference database for Wistar rats and C57/BL6 mice. Biol Chem 388:547–554
56. **Kaneko JJ** 1989 Clinical biochemistry of domestic animals, 4th ed. San Diego: Academic Press
57. **Karasawa H, Nagata-Goto S, Takaishi K, Kumagae Y** 2009 A novel model of type 2 diabetes mellitus based on obesity induced by high-fat diet in BDF1 mice. Metabolism 58:296–303
58. **Sleeman MW, Wortley KE, Lai KM, Gowen LC, Kintner J, Kline WO, Garcia K, Stitt TN, Yancopoulos GD, Wiegand SJ, Glass DJ** 2005 Absence of the lipid phosphatase SHIP2 confers resistance to dietary obesity. Nat Med 11:199–205